

Electrically-manipulable electron-momentum filter based on antiparallel asymmetric double δ-magnetic-barrier semiconductor microstructure

Ge Tang(唐鸽), Ying-Jie Qin(覃英杰), Shi-Shi Xie(谢诗诗), and Meng-Hao Sun(孙梦豪)

Citation: Chin. Phys. B, 2021, 30 (**10**): 107303. DOI: 10.1088/1674-1056/ac1570
Journal homepage: http://cpb.iphy.ac.cn; http://iopscience.iop.org/cpb

What follows is a list of articles you may be interested in

Accurate capacitance-voltage characterization of organic thin films with current injection

Ming Chu(褚明), Shao-Bo Liu(刘少博), An-Ran Yu(蔚安然), Hao-Miao Yu(于浩淼), Jia-Jun Qin(秦佳俊), Rui-Chen Yi(衣睿宸), Yuan Pei(裴远), Chun-Qin Zhu(朱春琴), Guang-Rui Zhu(朱光瑞), Qi Zeng(曾琪), and Xiao-Yuan Hou(侯晓远)

Chin. Phys. B, 2021, 30 (**8**): 087301. DOI: 10.1088/1674-1056/abe3e4

High-responsivity solar-blind photodetector based on MOCVD-grown Si-doped β-Ga_2O_3 thin film

Yu-Song Zhi(支钰崧), Wei-Yu Jiang(江为宇), Zeng Liu(刘增), Yuan-Yuan Liu(刘媛媛), Xu-Long Chu(褚旭龙), Jia-Hang Liu(刘佳航), Shan Li(李山), Zu-Yong Yan(晏祖勇), Yue-Hui Wang(王月晖), Pei-Gang Li(李培刚), Zhen-Ping Wu(吴真平), and Wei-Hua Tang(唐为华)

Chin. Phys. B, 2021, 30 (**5**): 057301. DOI: 10.1088/1674-1056/abe37a

Correlated insulating phases in the twisted bilayer graphene

Yuan-Da Liao(廖元达), Xiao-Yan Xu(许霄琰), Zi-Yang Meng(孟子杨), and Jian Kang(康健)

Chin. Phys. B, 2021, 30 (**1**): 017305. DOI: 10.1088/1674-1056/abcfa3

Self-powered solar-blind photodiodes based on EFG-grown (100)-dominant β-Ga_2O_3 substrate

Xu-Long Chu(褚旭龙), Zeng Liu(刘增), Yu-Song Zhi(支钰崧), Yuan-Yuan Liu(刘媛媛), Shao-Hui Zhang(张少辉), Chao Wu(吴超), Ang Gao(高昂), Pei-Gang Li(李培刚), Dao-You Guo(郭道友), Zhen-Ping Wu(吴真平), and Wei-Hua Tang(唐为华)

Chin. Phys. B, 2021, 30 (**1**): 017302. DOI: 10.1088/1674-1056/abc546

Probing the Majorana bound states in a hybrid nanowire double-quantum-dot system by scanning tunneling microscopy

Jia Liu(刘佳), Ke-Man Li(李科曼), Feng Chi(迟锋), Zhen-Guo Fu(付振国), Yue-Fei Hou(侯跃飞), Zhigang Wang(王志刚), Ping Zhang(张平)

Chin. Phys. B, 2020, 29 (**7**): 077302. DOI: 10.1088/1674-1056/ab8889

Electrically-manipulable electron-momentum filter based on antiparallel asymmetric double δ-magnetic-barrier semiconductor microstructure*

Ge Tang (唐鸽)[1], Ying-Jie Qin(覃英杰)[2,†], Shi-Shi Xie(谢诗诗)[2], and Meng-Hao Sun(孙梦豪)[2]

[1] College of Science, Shaoyang University, Hunan 422004, China
[2] College of Science, Guilin University of Technology, Guilin 541004, China

(Received 23 February 2021; revised manuscript received 18 June 2021; accepted manuscript online 18 July 2021)

We theoretically investigate the wave-vector filtering (WVF) effect for electrons in an antiparallel asymmetric double δ-magnetic-barrier microstructure under a bias, which can be fabricated experimentally by patterning two asymmetric ferromagnetic (FM) stripes on the top and the bottom of GaAs/Al_xGa_{1-x}As heterostructure, respectively. It is found that an appreciable WVF effect appears because of an essentially two-dimensional (2D) process for electrons across this microstructure. WVF effect is found to be sensitive to the applied bias. WVF efficiency can be tuned by changing bias, which may lead to an electrically-controllable momentum filter for nanoelectronics device applications.

Keywords: magnetic microstructure, bias, wave vector filtering (WVF) effect, electrically-tunable momentum filter

PACS: 73.40.−c, 75.47.−m, 73.40.Gk **DOI:** 10.1088/1674-1056/ac1570

1. Introduction

Advanced modern materials growth techniques (such as molecular beam epitaxy) make it possible to confine the motion of high mobility two-dimensional electron gas (2DEG) in a modulation-doped semiconductor heterostructure by an inhomogeneous magnetic field,[1] e.g., patterning a ferromagnetic (FM) stripe on the surface of GaAs/Al_xGa_{1-x}As heterostructure,[2] which allows to construct so-called magnetic microstructure in experiments.[3] In fact, magnetic microstructure consists of magnetic materials and semiconductor, where the former produces an inhomogeneous magnetic field affecting locally the motion of electrons in latter. Because of small size, low dimensionality and quantum magnetic confinement, some novel quantum effects exist in the magnetic microstructure,[4] e.g., wave-vector filtering (WVF),[5] magnetoresistance (MR) effect[6–9] and electron-spin polarization.[10–13] Meanwhile, these effects can be used to develop new nanoelectronics devices.[14–16]

Recently, WVF effect in magnetic microstructure has attracted much interest, owing to its scientific importance[17] and potential application.[18] Physically, such an effect results from an essentially two-dimensional (2D) process for electrons across magnetic microstructure.[5] In 2017, Lu *et al.*[19] firstly reported a theoretical study on WVF effect and its control via δ-doping in an experimentally-realizable magnetic microstructure. They found a considerable WVF effect, and confirmed that WVF efficiency can be controlled structurally by δ-doping. Since then, WVF effect in magnetic microstructures was explored extensively and corresponding electron-momentum filters were proposed successfully.[20–24]

More recently, an idea to confine 2DEG motion by an electric field, e.g., patterning Schottky-metal (SM) stripe on semiconductor heterostructure,[25,26] is put forward, in order to enhance manipulation to electron-momentum filter based on the magnetic microstructure. By depositing a FM stripe and a SM stripe on the top and the bottom of GaAs/Al_xGa_{1-x}As heterostructure, respectively, Liu *et al.*[27] found that this kind of magnetic microstructure also possesses an appreciable WVF effect and its efficiency can be altered by SM stripe. Ulteriorly, manipulating WVF effect by δ-doping and applied bias was investigated independently by Liu *et al.*[28] and Kong *et al.*,[29] respectively. Very recently, WVF effect[30] and influence of δ-doping[31] as well as applied bias[32] were studied in another such magnetic microstructure, where a FM stripe and a SM stripe were patterned, in parallel configuration, on the surface of GaAs/Al_xGa_{1-x}As heterostructure. These works not only revealed general rule of electric field controlled WVF effect in such magnetic microstructures, but also proposed the electrically-controllable electron-momentum filter for nanoelectronics device applications. By applying a bias, in the present work, we explore electric control to WVF effect for electrons in a magnetic microstructure, aiming at developing a new electrically-controllable electron-momentum filter for nanoelectronics device applications.

*Project supported by the National Natural Science Foundation of China (Grant No. 11864009).
†Corresponding author. E-mail: yijiqi20@126.com
© 2021 Chinese Physical Society and IOP Publishing Ltd

2. Model and method

We consider a magnetic microstructure[33] as plotted briefly in Fig. 1(a), where two asymmetric FM_1 and FM_2 stripes are patterned on the top and the bottom of GaAs/$Al_xGa_{1-x}As$ heterostructure,[34] respectively, and structural model is presented in Fig. 1(b). When vertical distance between FM stripes and 2DEG plane is very small as well as conductivity is identical everywhere within 2DEG, horizontally magnetized FM stripe induced magnetic fields and applied negative voltage ($-V_g$) produced electric potential can be viewed as[35] delta-function magnetic-barrier (MB) and rectangular electric-barrier (EB), respectively, i.e.,

$$\begin{cases} B_z(x) = B_1\delta(x) - B_2\delta(x-L), \\ U(x) = U_0, \quad 0 < x < L, \end{cases} \tag{1}$$

where $\delta(x)$ is Dirac delta-function, $B_{1,2}$ stands for magnetic strength of two δ-MBs, U_0 represents EB height, and L is structural width or separation between two δ-MBs.

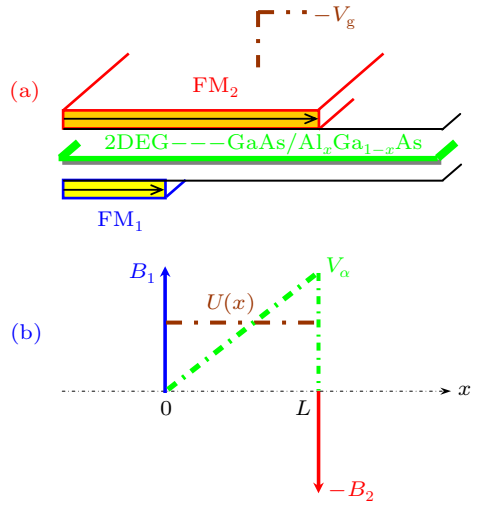


Fig. 1. (a) Magnetic microstructure and (b) its structural model with a bias.

At the presence of a bias (V_α), the Hamiltonian describing an electron in such a magnetic microstructure can be written, in the framework of single particle, effective mass approximation, by[36]

$$H = \frac{p_x^2}{2m^*} + \frac{[p_y + eA_y(x)]^2}{2m^*} + \frac{e\hbar g^*\sigma_z}{4m_0}B_z(x) + U(x) - \frac{eV_\alpha}{L}x, \tag{2}$$

where $\boldsymbol{p} = (p_x, p_y)$, $m^*(m_0)$, $-e$ and g^* are momentum, effective (free) mass, charge and effective Landé g-factor of an electron, respectively, and the magnetic vector potential is expressed, in Landau gauge, by $\boldsymbol{A}(x) = [0, A_y(x), 0]$ with

$$A_y(x) = \begin{cases} 0, & x < 0, \\ B_1\ell_B, & 0 < x < L, \\ (B_1 - B_2)\ell_B, & x > L, \end{cases} \tag{3}$$

where $\ell_B = \sqrt{\hbar/eB_0}$ is magnetic length. The third item in Eq. (2) is the Zeeman coupling, which is determined by the quantity $m^*g^*B_z/(4m_0)$. For GaAs material and $B_z = 1.5$ this item equals to 0.011,[37] therefore, the spin effect can be ignored.

For a magnetic microstructure, electron is free along the y-direction, solution of its stationary Schrödinger equation, $H\Psi(x,y) = E\Psi(x,y)$, can be therefore written by $\Psi(x,y) = \psi(x)\exp(\mathrm{i}k_y y)$, which k_y is wave vector in y-direction and x-component of wave function $\psi(x)$ complies with reduced one-dimensional (1D) Schrödinger equation

$$-\frac{\hbar^2}{2m^*}\psi''(x) + U_{\text{eff}}(x, k_y, V_\alpha)\psi(x) = E\psi(x), \tag{4}$$

with an effective potential felt by an electron in this magnetic microstructure

$$U_{\text{eff}}(x, k_y, V_\alpha) = \frac{[\hbar k_y + eA_y(x)]^2}{2m^*} - \frac{eV_\alpha}{L}x. \tag{5}$$

Clearly, this U_{eff} depends not only on wave vector (k_y), but also on bias (V_α). It is k_y-dependence of U_{eff} that renders an essentially 2D-process for electrons across a magnetic microstructure, leading to a WVF effect. The V_α-dependent U_{eff} makes possible control of WVF effect by an applied bias in a magnetic microstructure based electron-momentum filter.

The 1D Schrödinger equation (4) can be solved exactly by the transfer matrix method,[38] as in structural region wave function can be written, in the linear combination of the Hermitian functions.[39] In incident and transmitted regions, wave functions can be assumed by $\psi_{in}(x) = \exp(\mathrm{i}k_l x) + \gamma\exp(-\mathrm{i}k_l x), x < 0$ and $\psi_{out}(x) = \tau\exp(\mathrm{i}k_r x), x > L$, respectively, where $k_l = \sqrt{\frac{2m^*}{\hbar^2}(E - k_y^2)}$, $k_r = \sqrt{\frac{2m^*}{\hbar^2}[E + eV_\alpha - (k_y + B_1 - B_2)^2]}$ and γ/τ is reflected/transmitted wave amplitude. Matching these wave functions at $x = 0$ and L, one readily obtains transmission coefficient of electrons across this magnetic microstructure as

$$T(E, k_y, V_\alpha) = \frac{k_r}{k_l}|\tau|^2. \tag{6}$$

Then, WVF efficiency is evaluated by differentiating $T(E, k_y, V_\alpha)$ over k_y for given incident energy E,[19] i.e.,

$$\eta(E, k_y, V_\alpha) = \left.\frac{\partial T(E, k_y, V_\alpha)}{\partial k_y}\right|_E. \tag{7}$$

3. Results and discussion

In numerical calculations, all relevant quantities are written in dimensionless form, such as $E \to EE_0$, $x \to x\ell_B$, $B_z(x) \to B_z(x)B_0$ and $k_y \to k_y\ell_B^{-1}$, where $\ell_B = \sqrt{\hbar/eB_0}$ and $E_0 = \hbar eB_0/m^*$. For GaAs ($m^* = 0.067m_0$) and $B_0 = 0.2T$, $\ell_B = 57.5$ nm and $E_0 = 0.34$ meV. In order to highlight the effect of applied bias, we set $B_1 = 1.0$, $B_2 = 1.5$, $L = 3.0$ and $U_0 = 4.0$ throughout the whole paper.

We start with transmission coefficient for electrons traversing our considered magnetic microstructure. Figure 2 shows variation of transmission coefficient (T) with incident

energy (E) for wave vector $k_y = -0.5$ (solid curve), 0.0 (dashed curve) and +0.5 (dotted curve), where applied bias is set to be $V_\alpha = 3.0$. We can see clearly from this figure that electronic transmission through magnetic microstructure under a fixed bias as plotted in Fig. 1 is anisotropic with respect to wave vector k_y, namely, there is a significant difference of transmission between non-identical wave vectors. Such a characteristic originates from an essentially-2D process for electrons tunneling through magnetic microstructure or k_y-dependent effective potential ($U_{\rm eff}$) experienced by electrons in magnetic microstructure as indicated in Eq. (5), regardless of whether or not a bias is applied. Meanwhile, this difference of electronic transmission between wave vectors also implies that a considerable WVF effect still appears when our considered magnetic microstructure is applied by a bias. A controllable WVF effect is desired for electron-momentum filter. In the following, we examine detailedly the control of WVF effect by changing applied bias.

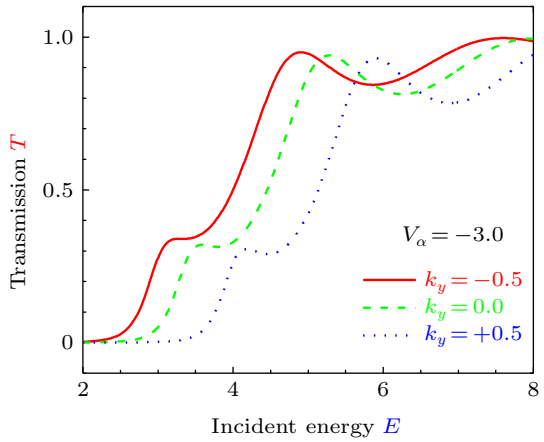


Fig. 2. Transmission coefficient changes with incident energy for different wave vectors and a fixed bias.

In Fig. 3, we present WVF efficiency (η) versus incident energy (E) for a fixed wave vector $k_y = 0.0$ (i.e., the normal incidence) and several concrete applied biases: $V_\alpha = 1.0$ (solid line), 2.0 (dashed line) and 3.0 (dotted line), respectively. One can observe from this figure that WVF efficiency η will be greatly altered if applied bias V_α changes. For considered energy range, WVF efficiency decreases obviously and its curve shifts to low-energy direction. Clearly, modulation of applied bias (V_α) to WVF effect stems from V_α-dependence of effective potential $U_{\rm eff}$ felt by electrons in magnetic microstructure.

In order to observe the modulation of applied bias on WVF effect more intuitively, in Fig. 4 we directly present change of WVF efficiency (η) with applied bias, where wave vector is still set to be $k_y = 0.0$, but incident energy is chosen as $E = 2.0$ (solid curve), 5.0 (dashed curve) and 8.0 (dotted curve), respectively. Indeed, it is true from this figure that an applied bias impacts on the WVF effect for electrons in the magnetic microstructure. Both magnitude and sign of WVF efficiency are dramatically altered with applied bias. Furthermore, the impact of an applied bias on WVF effect is related closely to incident energy, especially for incident energy $E = 5.0$ (see green line). Actually, influence of an applied bias to WVF effect attributes to the dependence of effective potential felt by electrons in the magnetic microstructure on the applied bias [cf. Eq. (5)], which makes possible the control of electron-momentum filter (see Fig. 1) by an applied bias and gives rise to an electrically-tunable electron-momentum filter.

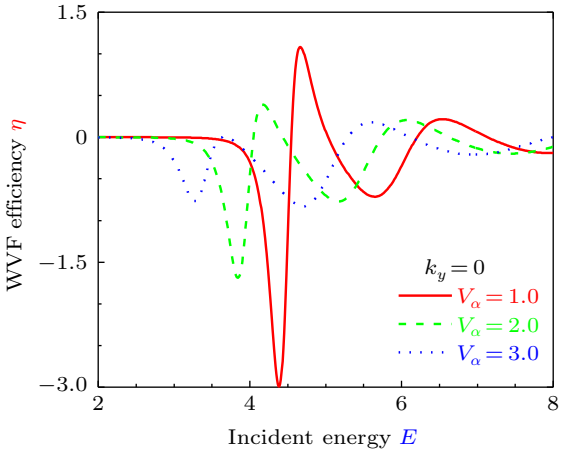


Fig. 3. WVF efficiency varies with incident energy under applied bias.

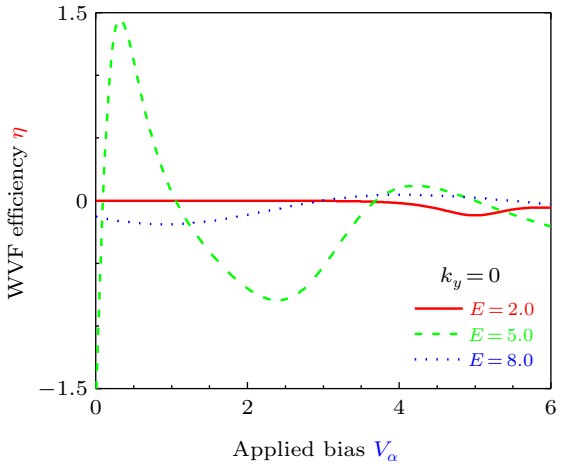


Fig. 4. WVF efficiency varies with incident energy under applied bias.

So far, the results are obtained only for one wave vector ($k_y = 0.0$). In order to observe the control of an applied bias to considered electron-momentum filter for different wave vectors, finally, Fig. 5 plots the WVF efficiency (η) as a function of applied bias (V_α), where three wave vectors are taken into account: $k_y = -0.5$ (solid line), 0.0 (dashed line) and +0.5 (dotted line), while incident energy is fixed at $E = 5.0$ for simplicity. From these (η–V_α) curves, we can see evidently that, an applied bias creates non-identical influence for different wave vectors on WVF effect for electrons to tunnel through the magnetic microstructure, especially at the case of $k_y = +0.5$. Such a difference originates from the dependence of effective potential ($U_{\rm eff}$) experienced by electrons in the magnetic microstructure on wave vector (k_y) [see Eq. (5)]. Thus, an applied

bias does impact on WVF effect in the magnetic microstructure for all of wave vectors.

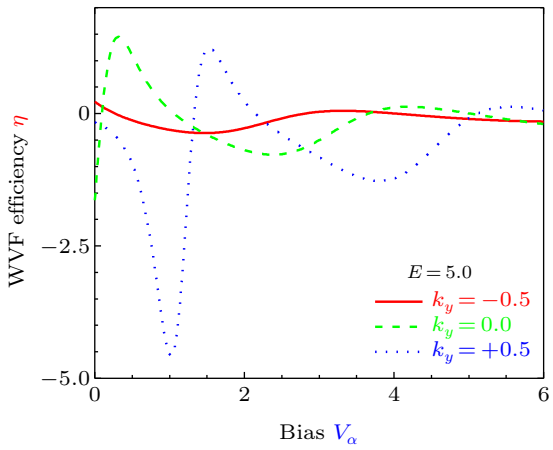


Fig. 5. WVF efficiency changes with applied bias for different wave vectors and fixed incident energy.

4. Conclusions

To sum up, control of WVF effect via an applied bias is investigated theoretically for electrons in a magnetic microstructure, which can be realized experimentally by depositing two asymmetric FM stripes on the top and the bottom of GaAs/Al_xGa_{1-x}As heterostructure, respectively. An appreciable WVF effect is revealed in such a magnetic microstructure under a bias, which attributes to an essentially-2D process for electrons across a magnetic microstructure, regardless of whether or not a bias is applied. Moreover, both magnitude and sign of WVF efficiency can be tuned by changing an applied bias, which may lead to an electrically-manipulable electron-momentum filter for nanoelectronics device applications.

References

[1] Tanaka M, Harbison J P, DeBoeck J, Sands T, Philips B, Cheeks T L and Keramidas B G 1993 *Appl. Phys. Lett.* **62** 1565
[2] Carmona H A, Geim A K, Nogaret A, Main PC, Foster T J, Henini M, Beaumont S P B and Blamire M G 1995 *Phys. Rev. Lett.* **74** 3009
[3] Matulis A, Peeters F M and Vasilopoulos P 1994 *Phys. Rev. Lett.* **72** 1518
[4] Nogaret A 2010 *J. Phys. Condens. Matter* **22** 253201
[5] Lu M W, Zhang L D and Yan X H 2003 *Nanotechnology* **14** 609
[6] Lu M W, Cao X L, Huang X H, Jiang Y Q and Yang S P 2016 *Appl. Surf. Sci.* **360** 989
[7] Jiang Y Q, Lu M W, Huang X H, Yang S P and Tang Q 2016 *J. Electron. Mater* **45** 2796
[8] Zhang L L, Lu M W, Yang S P and Tang Q 2016 *Phys. Lett. A* **380** 3520
[9] Liang D H, Lu M W, Huang X H, Huang M R and Cao Z L 2019 *Vacuum* **169** 108891
[10] Lu M W, Wang Z Y, Liang Y L and Li L Q 2013 *Appl. Phys. Lett.* **102** 022410
[11] Lu M W, Wang Z Y, Liang Y L and Li L Q 2013 *EPL* **101** 47001
[12] Lu M W, Cao X L, Huang X H, Jiang Y Q and Li S 2014 *J. Appl. Phys.* **115** 17430
[13] Lu M W, Cao X L, Huang X H, Jiang Y A, Li S and Yang S P 2015 *Superlattices Microstruct.* **77** 232
[14] Peeters F M and Li X Q 1998 *Appl. Phys. Lett.* **72** 572
[15] Governale M and Boese D 2000 *Appl. Phys. Lett.* **77** 3215
[16] Lu M W, Chen S Y, Huang X H and Zhang G L 2018 *IEEE J. Electron Dev.* **6** 227
[17] Zeng Z Y and Claro F 2002 *Phys. Rev. B* **65** 064207
[18] Papp G and Peeters F M 2004 *J. Phys. Condens. Matter* **16** 8275
[19] Lu M W, Chen S Y and Zhang G L 2017 *IEEE Trans. Electron. Dev.* **64** 1825
[20] Liu Y, Zhang L L, Lu M W, Zhou Y L and Li F 2017 *Solid State Commun.* **253** 6
[21] Liu X H, Liu C S, Gong Y J and Tang Z H 2017 *Philos. Mag. Lett.* **97** 150
[22] Zhang G L, Peng F F and Meng J S 2019 *J. Supercond. Nov. Magn.* **32** 451
[23] Chen S Y, Cao X L, Huang M R and Liang D H 2019 *Philos. Mag. Lett.* **99** 292
[24] Tang G, Liu G X and Ma W Y 2019 *Mod. Phys. Lett. B* **33** 1950421
[25] Liu G X, Zhang G L, Ma W Y and Shen L H 2016 *Solid State Commun.* **231-232** 6
[26] Zhai F, Xu H Q and Guo Y 2004 *Phys. Rev. B* **70** 085308
[27] Liu G X, Zhang L L, Zhang G L and Shen L H 2017 *Appl. Phys. A* **123** 241
[28] Liu X H, Liu C S, Xiao B F and Lu Y G 2018 *Vacuum* **148** 173
[29] Kong Y H, Lu K Y, He Y P, Liu X F, Fu X and Li A H 2018 *Appl. Phys. A* **124** 440
[30] Huang M R, Lu M W, Huang X H, Liang D H and Cao Z L 2020 *Mod. Phys. Lett. B* **34** 2050080
[31] Huang M R, Lu M W, Huang X H, Liang D H and Cao Z L 2020 *J. Supercond. Nov. Magn.* **33** 307
[32] Huang M R, Lu M W, Huang X H, Liang D H and Cao Z L 2020 *Vacuum* **180** 109580
[33] Lu M W and Yang G J 2007 *Phys. Lett. A* **362** 489
[34] Nogaret A, Bending S J and Henini M 2000 *Phys. Rev. Lett.* **84** 2231
[35] Papp G and Peeters F M 2001 *Appl. Phys. Lett.* **78** 2184
[36] Lu M W, Chen S Y, Zhang G L and Huang X H 2018 *J. Phys. Condens. Matter* **30** 145302
[37] Liang D H, Lu M W, Huang X H, Huang M R and Cao Z L 2019 *Vacuum* **169** 108891
[38] Cao Z L, Lu M W, Huang X H, Guo Q M and Yang S Q 2021 *Superlattices Microstruct.* **143** 106545
[39] Guo Y, Wang H, Gu B L and Kawazoe Y 2000 *Phys. Rev. B* **61** 1728